Morphologie du paysage agricole et liens avec la variabilité spatiale de l'épaisseur des sols

Ce chapitre comprend essentiellement un article accepté, sous presse, constituant *in extenso* le *§* III.2., dont les principaux résultats sont présentés et résumés dans le *§* III.1.

III.1. Objectifs et principaux résultats

Ce chapitre vise à **déterminer les relations existant entre certains éléments linéaires de la morphologie du site d'étude et la variabilité spatiale de l'épaisseur de sol**. Plus particulièrement, il sera recherché s'il y a des variations d'épaisseur de sol induites par des phénomènes de départ ou de dépôt de sol liés à la présence de bordures de parcelles. L'approche adoptée ici est focalisée plus particulièrement sur l'étude de figures morphologiques linéaires remarquables dans le paysage : ces figures sont principalement orientées perpendiculairement à la pente et de largeur décamétrique. Cette étude a fait l'objet d'un article, intitulé : « Classification and mapping of anthropogenic landforms on cultivated hillslopes using DEMs and soil thickness data – Example from the SW Parisian Basin, France », accepté et sous presse dans la revue "Geomorphology". Cet article comprend toutes les précisions sur les méthodes, les résultats et les interprétations.

Deux types de figures morphologiques linéaires ont été étudiés ici : les **banquettes agricoles** (« lynchets ») et les **ondulations** (« undulations »). Les premières sont actuellement associées à des bordures de parcelles, contrairement aux secondes. Les banquettes agricoles sont considérées comme des indicateurs topographiques de dépôt de sol (« topographic SEDI » ; *cf.* Ch. I). Des études ont montré que leur développement est assuré par l'effet de barrière induit par la bordure de parcelle associée, sur les flux de matière provenant de l'amont, flux d'origine hydrique et/ou aratoire (Bollinne, 1971; Papendick and Miller, 1977; Van Dijk *et al.*, 2005; Follain *et al.*, 2007). Une banquette agricole se caractérise sur le secteur étudié par une diminution progressive de pente en amont de bordure de parcelle,

menant à une pente très douce (< 3%), et par une rupture de pente large de quelques mètres en aval de la bordure (Fig. 3a et c de l'article *§* III.2.). Les ruptures de pentes associées aux banquettes L1, L2 et L3 (*cf. §* II.3.2.) peuvent engendrer localement une dénivellation de plus de 2 m. Les ondulations sont de larges convexités graduellement reliées à la pente générale du versant, à leurs parties amont et aval, par des concavités plus ou moins marquées (Fig. 3 b et d de l'article *§* III.2.). Six ondulations ont été observées sur le site d'étude (U1 à U6).

Un **MNA (Modèle Numérique d'Altitude)** a été établi sur une grille d'une maille régulière de 2 m sur le site d'étude de 16 ha afin de caractériser précisément sa morphologie (Fig. 6 de l'article *§* III.2.). La pente, la courbure profilée (verticale), la courbure planiforme (horizontale) et la courbure (Zevenberger and Thorne, 1987) ont été dérivées du MNA. L'épaisseur de sol, considérée comme la somme des épaisseurs des horizons L et S, a été densément prospectée sur le site d'étude (au total 734 sondages à la tarière à main sur les 16 ha). Pour ce faire, deux plans d'échantillonnage ont été adoptés (Fig. 4 de l'article *§* III.2.). Le plan d'échantillonnage Σ est raisonné : ces points se concentrent sur les trois banquettes et six ondulations observées sur le terrain. Le plan d'échantillonnage Δ suit un schéma aléatoire stratifié appliqué à l'ensemble du site d'étude (un point pris au hazard dans chacune des mailles de 25 m de côté d'une maille). L'épaisseur de sol a ensuite été estimée par krigeage sur le site total (Fig. 8a de l'article *§* III.2.) à partir d'un jeu d'estimation de 586 points (80% du jeu total). Les 148 points restant constituent un jeu de validation. La morphologie et l'épaisseur de sol sur le site d'étude montrent des schémas de variations communs. En effet, les variations à courte-distance de l'épaisseur de sol les plus marquées sont orientées perpendiculairement à la pente et concentrées sur les figures morphologiques étudiées.

Les **734 points de sondage ont alors éte répartis en trois classes, selon une méthode experte basée sur les variations de topographie** (*§* 2.3 et Fig. 5 de l'article *§* III.2.), en trois classes. La classe 1 contient les points situés sur les banquettes agricoles, la classe 2 ceux localisés sur des ondulations, et enfin la classe 0 regroupe les points en dehors des figures morphologiques (surfaces indifférenciées). Une **méthode de classification (« Classification Tree » : arbre de classification ; Breiman *et al.*, 1984)** basée sur des analyses statistiques a été appliquée au jeu d'estimation afin de construire automatiquement des modèles de classification des points dans les classes d'appartenance aux formes précitées. Deux modèles ont été construits. Le premier, nommé CT_{soil}, est basé sur l'analyse statistique

des variables prédictives suivantes : la pente, la courbure profilée, la courbure planiforme, la courbure, et l'épaisseur de sol. Le second utilise les mêmes variables prédictives, exceptée l'épaisseur de sol. L'efficacité de chacun des modèles est alors testée et discutée afin de souligner les liens existant entre figures morphologiques et variabilité spatiale de l'épaisseur de sol. Pour ce faire, chaque modèle a été implémenté dans le Système d'Informations Géographique ArcGIS 9.3 afin de cartographier les résultats de classification des figures morphologiques de chacun (Fig. 9 de l'article *§* III.2.). Chaque modèle permet d'identifier et de cartographier de manière plus ou moins précise les figures morphologiques étudiées à partir des variables prédictives concernées : les banquettes L1 à L3, et les ondulations U1 à U6. De plus, de nouvelles figures morphologiques linéaires et de largeur décamétrique sont détectées par les modèles CT_{topo} et CT_{soil}. Les résultats obtenus via la cartographie ont ensuite été comparés à la classification expert pour des points du jeu de validation.

Les résultats de validation des modèles CT_{soil} et CT_{topo} montrent respectivement que 83% et 67% des points du jeu de validation ont été correctement reclassés par ces modèles (Tab. 5 et 7 de l'article *§* III.2.). Chacun des deux modèles classe très bien les points situés sur les banquettes agricoles : ces figures ont en effet des caractéristiques morphologiques et d'épaisseur de sol très différentes des ondulations et des surfaces non différenciées. De ce fait, les gammes de valeurs de chacune des variables prédictives, morphologiques et d'épaisseur de sol de la classe 1 apparaissent statistiquement différenciables des gammes de valeurs observées en classes 0 et 2 (Tab. 3 de l'article *§* III.2.). Les principales erreurs observées dans l'application des deux modèles résident essentiellement de la difficulté de discriminer de manière nette les ondulations des surfaces indifférenciées (Tab.5 et 7 de l'article *§* III.2.). Il s'avère que les ondulations ne peuvent être distinguées des surfaces indifférenciées que sur la base des variables courbure, courbure profilée et épaisseur de sol (Tab. 3 de l'article *§* III.2.). Les confusions entre ondulations et surfaces indifférenciées sont donc plus marquées lorsque l'épaisseur de sol n'est pas prise en compte en tant que variable prédictive dans l'application d'arbre de classification (modèle CT_{topo}).

La variabilité spatiale de l'épaisseur de sol paraît plus importante au niveau des banquettes et des ondulations. En effet, ces figures morphologiques correspondent à des épaississements de sol. Les valeurs moyennes d'épaisseur de sol sont de 1,10 m, 0,62 m et 0,45 m, respectivement, dans les banquettes agricoles, les ondulations, et les surfaces

indifférenciées. La distribution spatiale des épaississements mesurés dans les figures morphologiques apparaît typique pour chaque type de figures. L'épaississement observé dans les banquettes agricoles évolue, en coupe verticale, comme un pseudo triangle rectangle (Fig. 8b de l'article *§* III.2.). L'épaississement de sol dans les ondulations évolue quant à lui plutôt avec la forme d'une lentille convexe (Fig. 8c de l'article *§* III.2.). La forme et l'intensité de ces épaississements de sol tendent à expliquer en grande partie la morphologie de chacune des figures prospectées. La variabilité spatiale du toit de la l'altérite du sous-sol (toit de l'horizon C) semble toutefois également intervenir de manière plus ou moins marquée dans l'intensité morphologique de certaines de ces figures.

La comparaison des cartes de classification obtenues et des réseaux parcellaires connus depuis 1836 démontre que les **ondulations** identifiées, et les épaississements de sol associés, sont **liés à des bordures de parcelles anciennes**, principalement disparues lors d'une campagne de remembrement de 1967. Les ondulations pourraient s'être développées à partir de processus d'érosion-dépôt liés à la présence prolongée d'une bordure de parcelle. Hypothétiquement, une ondulation pourrait correspondre à une ancienne banquette agricole, peu développée, et arasée lentement depuis 1967, date de disparition de la bordure (Bollinne, 1971 ; Houben, 2008). Une ondulation pourrait également correspondre à une « crête de labour » qui se forme par accumulation de sol, plus ou moins symétrique, de chaque côté d'une bordure de parcelle (Callot, 1980; Leturcq, 2008). Pour ce qui concerne les banquettes agricoles du site d'étude, bien marquées dans le paysage et identifiées par les modèles, elles semblent quant à elles associées à des bordures pérennes depuis au moins 1836.

Au total, banquettes agricoles et ondulations couvrent 39% de la surface totale du site et stockent pratiquement 15% du volume total de sol présent sur le site. Comme les banquettes agricoles, les ondulations semblent apparaître comme des indicateurs topographiques d'érosion-dépôt de sol induits par les parcellaires agricoles anciens. Cette étude permet de souligner l'importance des parcellaires actuels et anciens sur la variabilité spatiale actuelle de l'épaisseur des sols sur le site d'étude. Elle ouvre également de nouvelles perspectives sur les possibilités de dresser des cartes prédictives de l'épaisseur des sols, et donc de certaines de leurs propriétés, à partir des paramètres des figures morphologiques associées au parcellaire en contexte agricole.

Les figures morphologiques linéaires traduisent donc des variations d'épaisseur de sol. La question se pose de la cause de ces variations : les matériaux constituant les sols ont-ils subi un transport (sols autochtones ou allochtones) ? et si oui, quel en est l'agent (hydrique ou aratoire) et depuis quand ? Ces questions seront traitées dans les chapitres suivants.

III.2. Article accepté, sous presse dans « Geomorphology »

Classification and mapping of anthropogenic landforms on cultivated hillslopes using DEMs and soil thickness data – Example from the SW Parisian Basin, France

Chartin, C. [a,*], Bourennane, H. [b], Salvador-Blanes, S. [a], Hinschberger, F. [a], Macaire, J.-J. [a]

[a] *Université François-Rabelais de Tours, Université d'Orléans, CNRS/INSU, Institut des Sciences de la Terre d'Orléans - UMR 6113, Faculté des Sciences et Techniques, Parc Grandmont, 37200 Tours, France*

[b] *INRA - Unité de Science du Sol, 2163 avenue de la Pomme de Pin, CS 40001 Ardon, 45075 Orléans Cedex 2, France*

***** Corresponding author: Tel. +33/2/47367339, Fax. +33/2/47367090

E-mail address: caroline.chartin@etu.univ-tours.fr (C. Chartin)

Abstract

This study focuses on linear anthropogenic landforms of decametric width on cultivated hillslopes and their relations to soil thickness variability. The 16 ha study area shows a rolling topography supported by Cretaceous chalk of the SW Parisian Basin, France. Two types of landforms were identified: lynchets, similar to those described as soil terraces occurring on downslope field parts in other contexts, and undulations, linear, convex landforms that cut across fields. An accurate DEM and a detailed soil thickness survey were performed all over the study area. Soil samples were classified considering their location on specific types of anthropogenic landforms. Classification tree (CT) method was applied to assess whether lynchets and undulations can be discriminated through morphometric attributes (slope,

curvature, profile curvature and planform curvature) and soil thickness (CT_{soil}) or through morphometric attributes only (CT_{topo}). The CT application establishes predictive classification models to map the spatial distribution of lynchets and undulations over the whole study area. The validation results of the CT_{soil} and CT_{topo} applications show model efficiencies of 83% and 67%, respectively. Both models performed well for lynchets. Errors arise mainly from difficulties in unequivocally discriminating gently convex undulations and undifferentiated surfaces, especially when soil thickness is not accounted for. Mean values of soil thickness are 1.08, 0.62 and 0.45 m in lynchets, undulations and undifferentiated areas, respectively. The general shape of the thickened soil is characteristic to each type of anthropogenic landform. Multi-temporal mapping of field border networks shows that undulations are linked to borders that were removed during the latest land consolidation. Lynchets are associated with current field borders. Lynchets and undulations, which cover 39% of the study area, define topographic indicators of human-induced soil accumulations. The method involves perspectives for efficiently mapping and quantifying the anthropogenically modified spatial variability of soil thickness on agricultural hillsides.

Keywords: Digital Elevation Model; Morphometric attributes; Soil thickness; Lynchet; Field borders; Classification Tree.

1. Introduction

The thickness and horizonation of soil cover result from the interaction of soil forming processes through parent-rock weathering and erosion or accumulation of matter at the soil surface (e.g., Jenny, 1941; Huggett, 1997). Accordingly, the thicknesses of the A and B horizons, as well as solum thickness are important diagnostic features for soil classification schemes (e.g., FAO, 1998). Moreover, soil properties such as water storage capacity and carbon content are sensitive to thickness variations (Van Wesemael *et al.*, 2000; Yoo *et al.*, 2006; Follain *et al.*, 2007). Soil thickness variation has a direct impact on crop quality and yields on cultivated land (Power *et al.*, 1981; Christensen and McElyea, 1988; Kosmas *et al.*, 2001). Recording soil thickness in agrarian landscapes, therefore, appears to be important for soil mapping.

Soil thickness is strongly linked to landscape morphology. Slope gradient is a major factor for soil development because it affects soil stability against gravity-induced movements (soil creep, landslide and debris flows) and controls rill and interrill erosion (Gerrard, 1981; Vandaele *et al.*, 1996; Chaplot and Le Bissonnais, 2000). The notion of landscape is predominated by the assumption of spatial heterogeneity that includes patterning or structuration (Turner *et al.*, 2001; Farina, 2006; Bolliger *et al.*, 2007). Meeus *et al.* (1990) defined agricultural landscapes as areas where "management is manifest and the interaction of such factors as soil conditions, elevation, use, management and history are visible in the landscape and are expressed in its form and layout". Few contiguous fields or several hundred hectares dedicated to agricultural practices can define an agricultural landscape. Landscape morphology primarily depends on natural parameters: tectonics, lithology and climate (Derruau, 1962). In addition to natural factors, human activities can significantly affect geomorphology. Anthropogenic deforestation often induces a significant increase in soil erosion (de Moor *et al.*, 2008, Macaire *et al.*, 2010). Landscape fragmentation by field border networks has also important effects on the spatial variability of soil erosion (Van Oost *et al.*, 2000; Follain *et al.*, 2006; Szilassi *et al.*, 2006). The spatial variability of tillage erosion is affected by field geometry as soil translocation by tillage implements occurs exclusively within field limits. Field borders act then as barriers to soil matter fluxes for tillage translocation, and also to fluxes for water translocation when borders are vegetalised (Dabney *et al.*, 1999; Govers *et al.*, 1999; De Alba, 2003; Van Dijk *et al.*, 2005; Knapen *et al.*, 2008). This leads to the formation of anthropogenic landforms that relate to local soil erosion/accumulation such as ridges-and-furrows, headlands, and lynchets that are frequently found in Western Europe (Callot, 1980; Hooke, 1988; Zadora-Rio, 1991; Houben, 2008). These features can be unintentional or intentional, when they are used for soil and water conservation systems (ridges-and-furrows, lynchets) or as biodiversity conservation systems (headlands) (Taylor, 1975; Corbet, 1995; Bellemlih, 1999).

In soil science and geomorphology, lynchets provide an example of an anthropogenic landform resulting from agricultural practices. Lynchets are also known as terraces, soil banks or fence lines. They are locally called "rideaux" in northern France and Belgium. A lynchet is predominantly shaped by the progressive accumulation of soil material by water and/or tillage translocation upslope of a field border (Bollinne, 1971; Papendick and Miller, 1977; Van Dijk *et al.*, 2005; Follain *et al.*, 2007). This leads to the creation of a gentler slope than in the

upslope field area and an associated break-in-slope below the field border. Depending on the slope gradient upslope and the degree of development of the lynchet, the break-in-slope can range from several decimetres to a few meters height (Papendick and Miller, 1977; Salvador-Blanes *et al.*, 2006). Moreover, the benching effect tends to be amplified by erosion downslope of the break-in-slope (Van Oost *et al.*, 2000; Follain *et al.*, 2007). Although lynchets are of decametric width, they may store an important proportion of soil material on cultivated hillslopes because of their frequent occurrence in the landscape (Macaire *et al.*, 2002).

Previously cited studies suppose that the lynchets could reflect different degrees of development and quantities of accumulated soil material depending on their morphometric attributes. Whereas relief was demonstrated as a useful and dominant predictive variable on the spatial distribution of soils and associated thicknesses (e.g., Huggett, 1975; Bourennane, 1997; Heimsath *et al.*, 1999; King *et al.*, 1999), few studies linked mathematically the morphologies of the anthropogenic features to their associated soil thicknesses. The easy acquisition of elevation data for large-scale areas makes its use very common for soil mapping (Odeh *et al.*, 1994; Gessler *et al.*, 1995; Isambert *et al.*, 1997; Grinand *et al.*, 2008).

The objective of this paper is to assess whether different types of anthropogenic landforms can be discriminated by their morphometric attributes and soil thicknesses. We proceeded to obtain accurate elevation records and conducted a detailed soil thickness survey with two different sampling strategies on anthropogenic landforms and undifferentiated surfaces. We developed a method to classify soil samples considering their location on or outside of specific types of anthropogenic landforms. We then executed predictive modelling of the belonging of a sample to the different types of anthropogenic landforms or surrounding undifferentiated surfaces using classification tree (CT) analysis (Breiman *et al.*, 1984). Results were analysed to assess the statistical relevance of morphological and soil thickness differences between types of anthropogenic landforms and with undifferentiated surfaces. Finally, we examined the influence of landscape fragmentation on the anthropogenic landforms and the convenience of using this method for soil quantification and mapping.

2. Materials and methods

2.1. Study area

2.1.1. Location and physiographical settings

The field study was carried out on a 16 ha southeast-facing hillslope located near the village of Seuilly within the Quincampoix catchment (southwestern Parisian Basin, 47°08.31'N, 0°10.97'E; Fig. 1). The elevation of the study area ranges from 37 to 80 m, and the slope is approximately 750 m. This hillslope has a rolling topography that is representative of the Upper Cretaceous formations of the southwestern Parisian Basin bedrocks. The studied hillslope is composed of the following sedimentary bedrocks from thalweg to crest: Upper Cenomanian sandy marl, Lower and Middle Turonian white chalks, and Upper Turonian yellow sandy limestones (Alcaydé *et al.*, 1989; Bellemlih, 1999). The main soils observed in this area are calcaric Cambisols, epileptic calcaric Cambisols and colluvic Cambisols (Boutin *et al.*, 1990; FAO, 1998; Bellemlih, 1999).

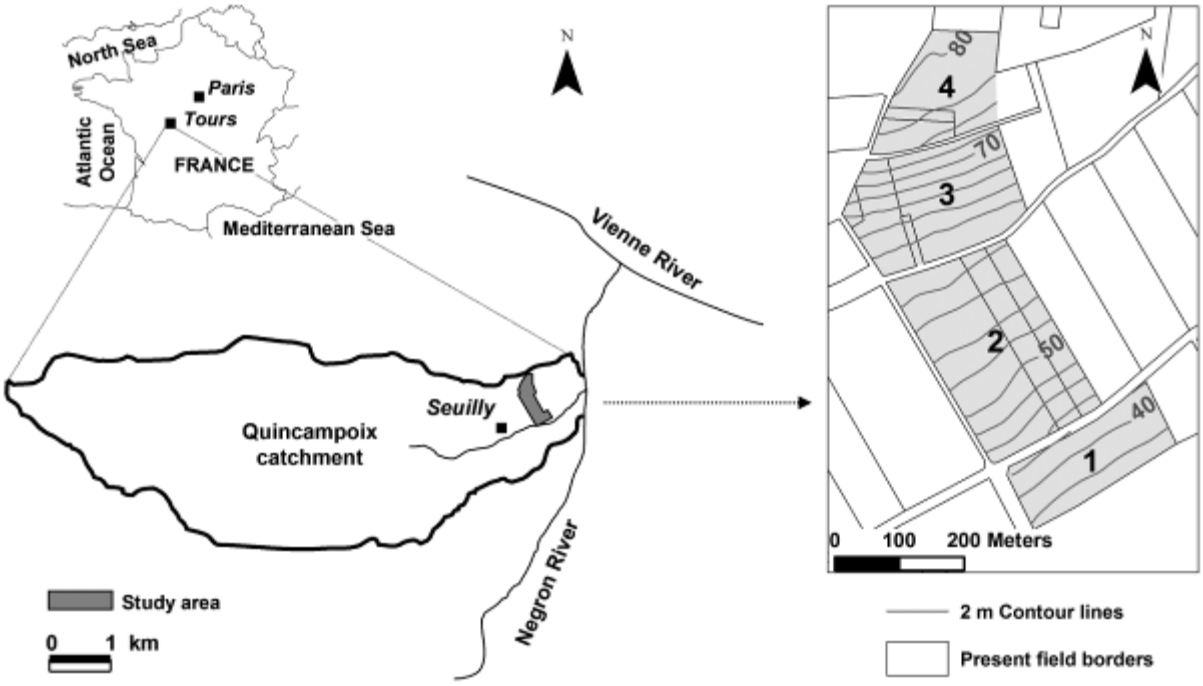

Figure 1. Location and topography of the study area.

Modern land-use consists of cultivated cereals and oil-producing crops (maize, wheat, barley, sunflower and rape). Vineyards, orchards and pastures covered over 30% of the study area until the beginning of the last century. The field border network has evolved remarkably since 1836 but has not changed since the last important land consolidation occurred at the end of the 1960s (Fig. 2).

2.1.2. Characteristics of the anthropogenic landforms in the study area

Lynchets and undulations are two types of linear anthropogenic landforms that have been identified in the study area. Their axes are predominantly oriented at right angles to the main slope direction.

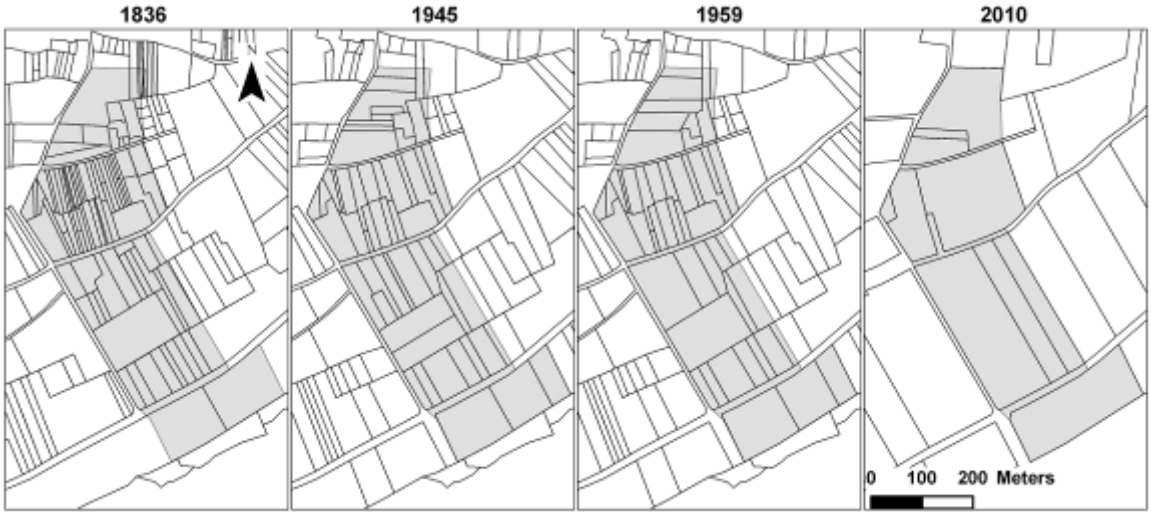

Figure 2. Field border networks in 1836, 1945, 1959 and 2010.

Fig. 3a,c shows the geometrical characteristics of a typical lynchet. It is characterised by two morphological components separated from one another by a field border, i.e., its axis. The first morphological component corresponds to a gentle slope extending a few decametres upslope of the axis. This gentle slope becomes gradually higher to connect to the upslope field area and tends to become close to zero when reaching the field border downslope. The second component is a few-meters wide break-in-slope located downslope of the axis. Breaks-in-slope can locally be more than 2 m high and create sharp discontinuities in the studied hillslope. Some augerings were carried out in the study area during a previous study

(Bellemlih, 1999). These augerings show soil thickening in the lynchets: soil thicknesses ranged from 75 to 130 cm in lynchets compared to 40 cm to >1 m in surrounding areas.

Fig. 3b,d shows the geometrical characteristics of the undulations. They do not create sharp discontinuities between both sides of the axis in landscape morphology. An undulation consists of a wide gentle convexity that is gradually connected at its external parts to the general hillslope morphology. The upslope and downslope connections mainly appear as a slight slope gentling of landscape. The tops of convexities are considered as the axes of undulation landforms.

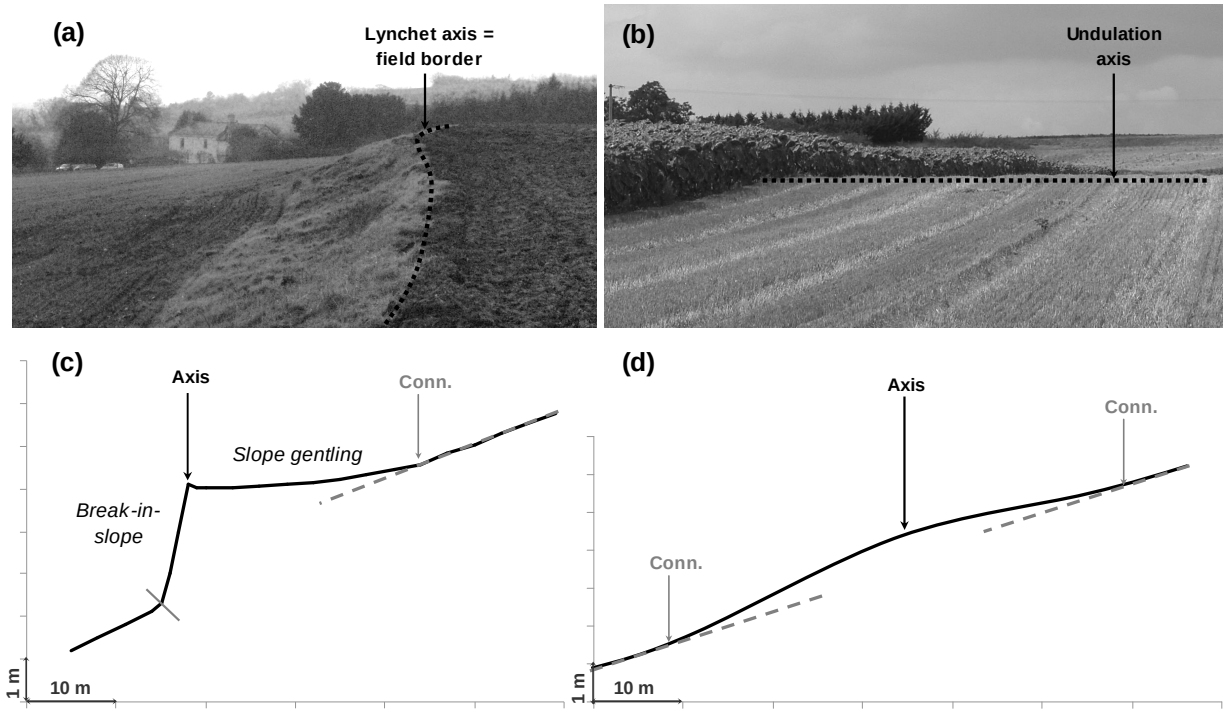

Figure 3. Illustrations of the two types of linear anthropogenic landforms present in the study area: (a) and (c) present a view and a topographic cross-section of a lynchet; (b) and (d) present a view and a topographic cross-section of an undulation ("conn." : connection).

2.2. Data acquisition

2.2.1. Topography

Two DGPS (Trimble ® ProXRS) were used as a base and a mobile recorder, respectively. Coordinates (accuracy in x,y: few millimetres) and elevations (accuracy in z:

approximately one centimetre) of 1550 points were obtained by data post-treatment. Four digital elevation models (DEMs) were produced independently on a 2-m grid, i.e., one DEM for each area delineated by lynchet breaks-in-slope (noted 1 to 4 in Fig. 1). The partitioning of the dataset into four subsets was added to the mapping procedure to avoid levelling of the lynchets when computing the DEMs. This virtual levelling would indeed imply a weak predictive power of the morphometric attributes derived from the DEMs. Finally, slope, profile curvature, planform curvature and curvature were derived from each DEM. The curvature was calculated using an algorithm developed by Zevenbergen and Thorne (1987).

2.2.2. Soil thickness

Soil thickness was measured by manual augering and defined as the summation of A and B horizons, i.e., the depth of the upper saprolite limit. Differentiation between B and C horizons was relatively easy because C horizons are white and the transition is sharp. As proposed by Follain *et al.* (2006), two sampling schemes were established to consider short-distance variability of soil thickness, especially the variability associated with linear anthropogenic landforms (Bolline, 1971; Macaire *et al.*, 2002; Salvador-Blanes *et al.*, 2006). The two sampling schemes were defined as follows:

Sampling Σ: 502 soil augerings were carried out on the nine most relevant linear landforms observed in the study area, i.e., three lynchets and six undulations (L1 to L3 and U1 to U6 for lynchets and undulations, respectively; Fig. 4a). The augerings were conducted regularly along transects that were either longitudinal or perpendicular to the landform axes (Fig. 4a). Longitudinal transects correspond to landform axes where one augering was performed every 8 m (Fig. 4b). A perpendicular transect crosses each longitudinal transect every 40 m. There is one augering every 4 m along the perpendicular transects.

Sampling Δ: 232 additional soil augerings were performed to precise the variation of soil thickness all over the study area. A point was sampled randomly in each square of a 25×25 m grid over the whole study area (Fig. 4a).

Both sampling schemes represent a total of 734 points. Twenty percent of the observations (148 points) were randomly selected to constitute the validation set. The

remaining 80% of the dataset (586 points) was used as the calibration set. Then, these 586 points were used to estimate soil thickness over the entire study area using ordinary kriging (e.g., Goovaerts, 1997; Chilès and Delfiner, 1999). The estimation of soil thickness, named STh_1, was performed over a 2-m regular grid considering the short-distance variation of soil thickness within lynchets and undulations.

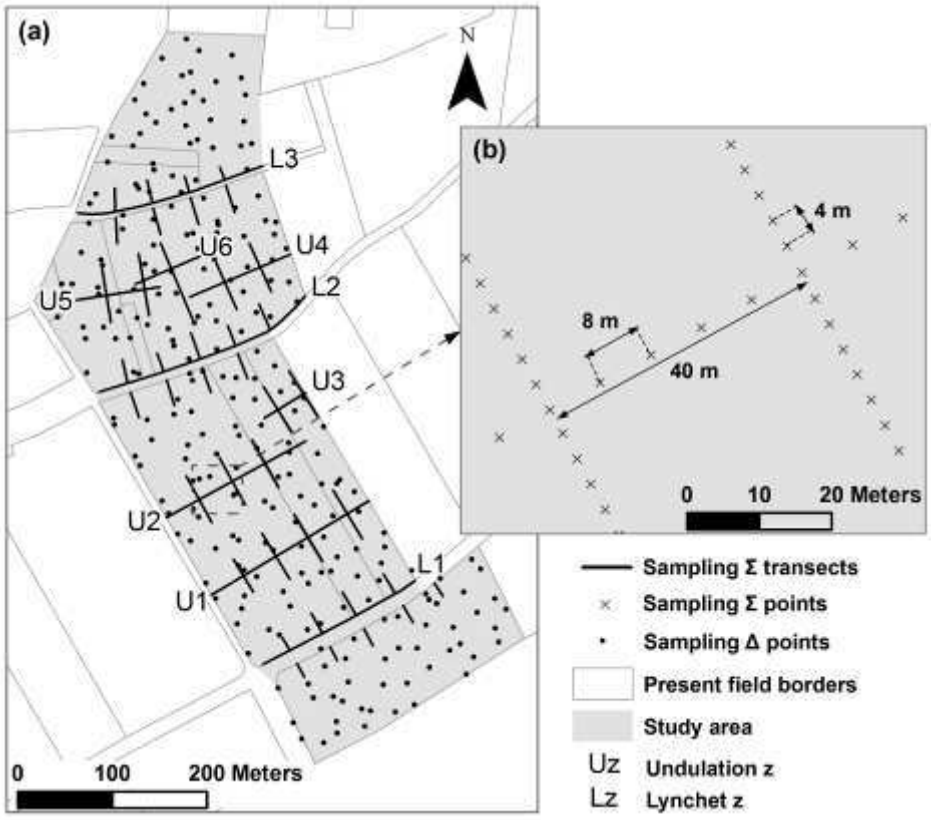

Figure 4. Soil sampling schemes: (a) samplings Σ and Δ in the whole study area; (b) zoom on sampling Σ scheme in an undulation (U2).

2.3. Expert classification method

The expert classification method consists of attributing each sampling point to one of the three predefined classes. Class 1 contains all points located on identified lynchets. Class 2 corresponds to points located on identified undulations. Finally, class 0 is "a class by default" that contains points located on undifferentiated surfaces. The expert classification was based on sample location and landform variation in close neighbourhoods. Datasets of sampling Σ and sampling Δ were treated separately.

2.3.1. Sampling Σ classification

The sampling scheme Σ was constructed using longitudinal and perpendicular transects located on the studied linear landforms (Fig. 4). Points sampled along longitudinal transects, i.e., along the landform axes, were automatically classified in class 1 for those located on lynchets and in class 2 for those located on undulations.

Fig. 5 presents an illustration of the expert classification for the perpendicular transects. Areas located downslope of breaks-in-slope were not considered as parts of lynchet landforms. Thus, points sampled downslope of lynchet axes along perpendicular transects were automatically attributed to class 0 (Fig. 5a). For the perpendicular transects located upslope of a lynchet axis and the whole perpendicular transects located on undulations, we defined the points of connection between linear anthropogenic landforms and the surrounding relief (Cf. Section 2.1.2). Then, samples located between the axis of the landform and points of connection were placed in class 1 for lynchets and class 2 for undulations. Points located between connections and transect extremities were placed in class 0, corresponding to undifferentiated surfaces.

2.3.2. Sampling Δ classification

Sampling Δ was dispatched all over the study area (Fig. 4a). For each point close to a lynchet or an undulation, a topographic cross-section perpendicular to the feature axis and crossing the point was extracted from the DEM using ArcGIS 9.3 ®. The classification method was similar to the one applied to points placed along perpendicular transects of sampling scheme Σ (Section 2.3.1). All points located on undifferentiated surfaces were attributed to class 0.

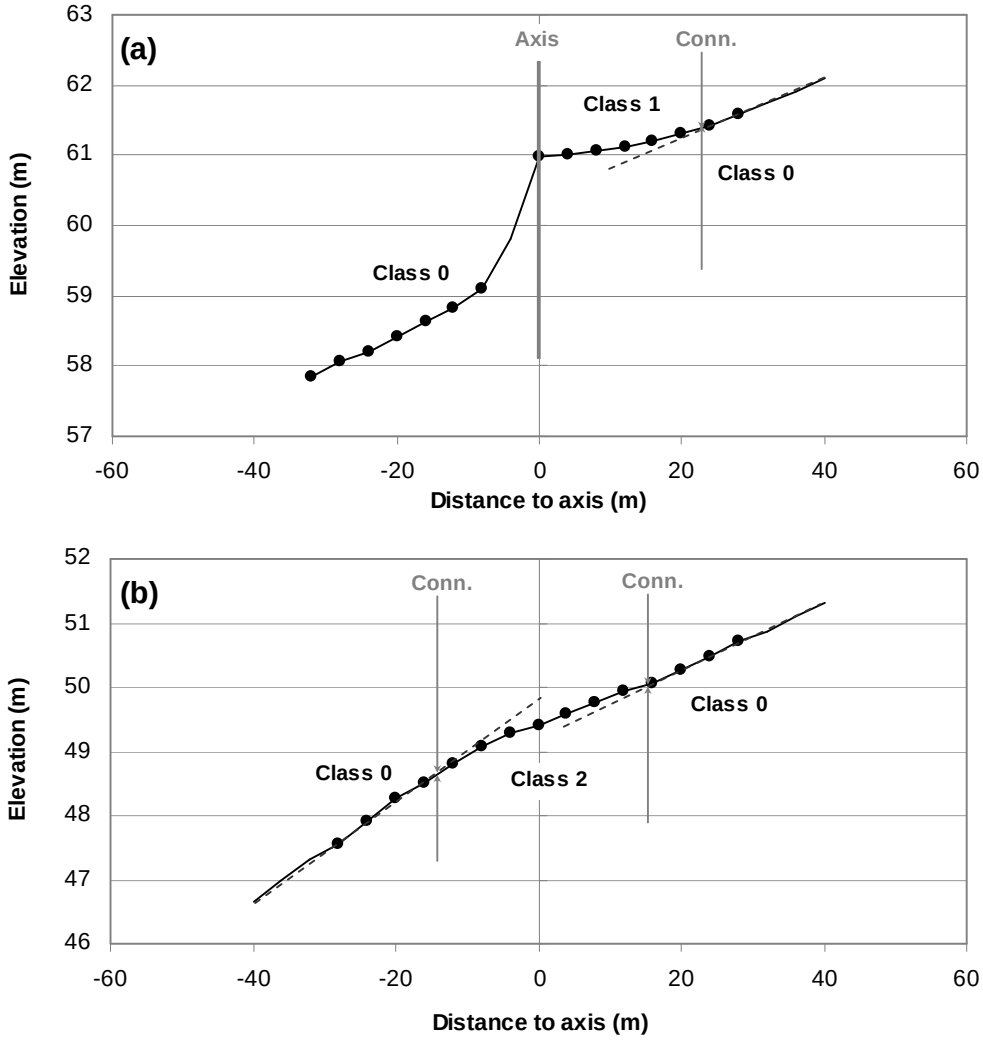

Figure 5. Illustrations of the classification method for perpendicular transects of soil sampling scheme Σ: (a) perpendicular transect on a lynchet and (b) on an undulation (dots: soil samples locations, "conn." : connection).

2.4. Statistical analyses

2.4.1. Principle of the Classification Tree (CT) method

This subsection briefly presents the Classification Tree (CT) method used for the main objective of this study. The convenience of this approach compared to discriminant analysis or logistic regression lies in its non-parametric character (no assumption is required regarding the distribution of the used variables). Several studies have already shown that CT method is useful for soil attribute prediction and mapping (e.g., Lagacherie, 1992; Shatar and

McBratney, 1999; McBratney *et al.*, 2003). For a thorough presentation of the CT method, readers should refer to books such as those by Breiman *et al.* (1984) or Steinberg and Colla (1995).

A CT corresponds to a model that predicts the class belonging of an object from values of one or more predictor variables (categorical and/or continuous). The tree is built from a calibration dataset; the class belonging and the predictor variables are known for each object of the set. A decision algorithm that partitions into increasingly homogeneous subdatasets is applied to this calibration dataset. At each successive partition, the decision algorithm automatically determines the splitting predictor variables and their values to minimize the variance between the parent dataset and its child subdatasets. When partitioning is achieved, each object from the calibration dataset has been sent to a terminal subdataset assigned to one of the predefined classes (several terminal datasets can be assigned to the same class). Thus, the built tree or 'classification model' consists of a rules-structured classifier. Decision rules follow one another in a fixed order and are based on values of the chosen predictor variables. We applied the Classification And Regression Tree (CART) algorithm developed by Breiman *et al.* (1984) that generates a binary decision tree. Data are partitioned into a series of descending left and right sub-datasets. This partitioning is recursive; thus, a defined predictor can be used in more than one decision rule.

2.4.2. Applications of the Classification Tree method

Here, we first applied the CART algorithm (R Development Core Team, 2010) to the 586-point calibration dataset. This set was previously classified into the three predefined classes 0, 1 and 2 through our expert method (Section 2.3). The predictor variables were the morphometric attributes (slope, curvature, profile curvature and planform curvature) and the soil thickness measured in the field. The resulting tree was called 'CT_{soil}'. In order to validate this classification model (CT_{soil}), we proceeded to the mapping of lynchet and undulation landforms all over the study area based on the decision rules of the model. For this purpose, each raster layer corresponding to morphometric attributes and soil thickness (STh_1) was previously computed over the same regular 2-m grid. Then, we implemented the decision rules of CT_{soil} into ArcGIS 9.3 ® and applied them for classifying each cell of the 2-m grid into one of the predefined classes 0, 1 or 2. When values of the predictor variables did not

correspond to any criteria imposed by CT_{soil}, the relative cell was automatically classified into class 0. Once the map was computed, the validation of the CT_{soil} model was carried out through the validation dataset. A class was attributed to each point of the validation dataset according to the map and compared with the initial expert classification.

For the purpose of spatial extrapolation beyond areas where soil thickness variable is unavailable, the CART algorithm was tested using only morphometric attributes as predictor variables. This application could constitute a practical tool for the identification and mapping of anthropogenic landforms when soil thickness is unknown or partially known in an area. The resulting classification model was referred to as 'CT_{topo}'. The methodology for the validation of the model was similar to the one applied to CT_{soil}.

2.5. Quantification of soil material stored in anthropogenic landforms

We quantified the soil material potentially stored in the anthropogenic landforms revealed by the most efficient classification model amongst CT_{soil} and CT_{topo}. We applied a method substracting the estimation of soil thickness that does not include soil material stored in the anthropogenic landforms (STh_2) to the estimation of actual soil thickness (STh_1). We took the following steps for this purpose:

(i) STh_2 was computed over the study area using only soil thickness measurements at points belonging to expert class 0.

(ii) A third raster layer was calculated as follows: $STh_{st} = STh_1 - STh_2$. It represents the storage soil thickness t_i for a given cell of the regular 2-m grid.

(iii) The total volume of soil material stored in each type of landform was calculated separately using Eq. (1):

$$V_{st}(m^3) = \sum_{i=1}^{n} (t_i \times ea) \qquad (1)$$

where i is the ith cell for a given landform type, n is the total number of cells of a given landform type, t_i is the storage soil thickness for the ith cell given by STh_{st} (m), and ea is the cells elementary area (2 m x 2 m).

3. Results

3.1. Variability of the predictor variables within the study area

Table 1 summarises statistics of morphometric attributes and measured soil thicknesses for the total 734 sampled points distributed over the entire study area. Slope shows a mean value of 5.3% with respective minimum and maximum values of 0.16% and 11.9%. The three different types of curvature present mean values close to null. Curvature presents a wider range of values from −1.00 to 1.18 m^{-1} when compared to profile and planform curvatures. Ranges of profile and planform curvature values are very distinctive; profile curvature varies from −0.97 to 1.03 m^{-1}, and planform curvature varies from −0.32 to 0.47 m^{-1}. As observed in field, data reflect that the most important short-distance variations of slope gradient are oriented towards the maximum slope direction, perpendicularly to the axes of studied lynchets and undulations (Fig. 6).

Table 1. Summary statistics of morphometric attributes and soil thickness calculated from the total dataset of 734 points.

Variable	Unit	Min	Mean	Max	S.D.**
Slope	%	0.16	5.31	11.90	1.53
Curvature*	m^{-1}	-1.00	-0.03	1.18	0.19
Profile curvature*	m^{-1}	-0.97	0.03	1.03	0.17
Planform curvature*	m^{-1}	-0.32	0.00	0.47	0.07
Soil thickness	m	0.22	0.62	2.23	0.33

* The negative values of curvature and planform curvature mean for concavity and positive values for convexity. The negative values of profile curvature mean for convexity and positive values for concavity.

** S.D: Standard Deviation.

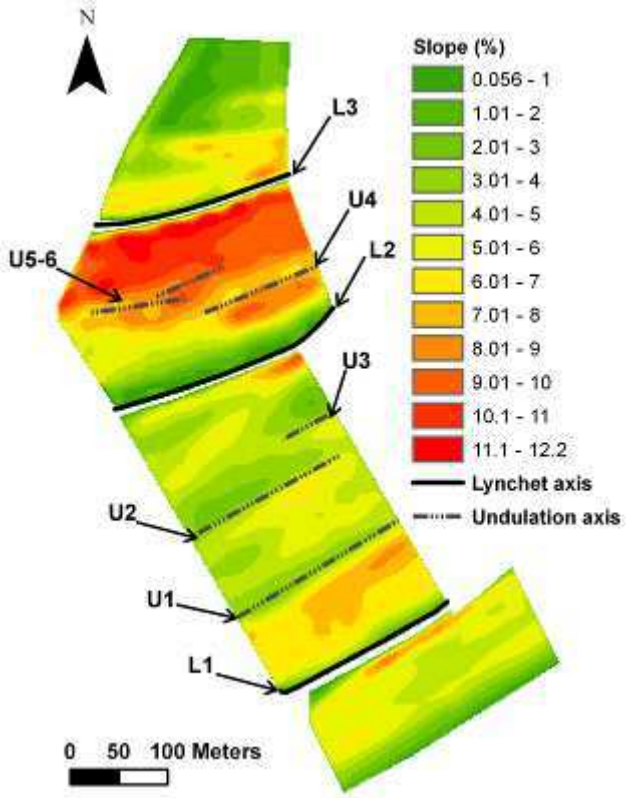

Figure 6. Map of slope gradient within the study area and location of lynchets and undulations axis.

Soil thickness measured in the field ranges from 0.22 to 2.23 m for the total dataset (Table 1). The mean measured value is 0.62 m with a standard deviation (S.D.) of 0.33 m. From the calibration dataset of 586 points, soil thickness was estimated over the entire study area by ordinary kriging. The spatial autocorrelation of soil thickness, quantified through the semi-variogram, is quite strong (Fig. 7). A pure nugget (sill = 0.01 m^2) plus a Gaussian model (range = 35 m and sill = 0.05 m^2) and a spherical model (range = 150 m and sill = 0.03 m^2) were nested to the experimental variogram. A cross validation was used on the original data to validate the variogram models. The mean error is defined as:

$$R = \frac{1}{n}\sum_{i=1}^{n}\left[z^*(\mathbf{x}_i) - z(\mathbf{x}_i)\right], \qquad (2)$$

where $z^*(x_i)$ is the estimated value at x_i, and $z(x_i)$ is the measured value at x_i.

R appears close to zero (-0.00117 m). The ratio of the mean squared error to the kriging variance is:

$$S_R^2 = \frac{1}{n}\sum_{i=1}^{n}\left[z^*(\mathbf{x}_i) - z(\mathbf{x}_i)\right]^2 / \sigma^2{}_k(\mathbf{x}_i), \qquad (3)$$

where $\sigma^2_k(x_i)$ is the theorethical estimation variance for the prediction of $z^*(x_i)$.

The ratio is close to unity (1.01628). The short-distance variability of soil thickness appears to be predominantly associated with all the lynchets, L1, L2 and L3, and undulations, especially U2, U4, U5 and U6 (Fig. 8a).

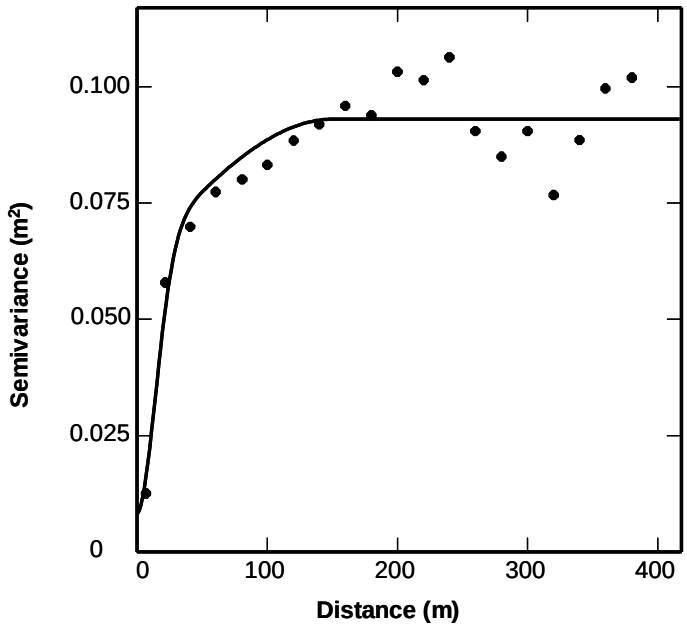

Figure 7. Experimental variogram of soil thickness (dots) and the theoretical model fits (solid line).

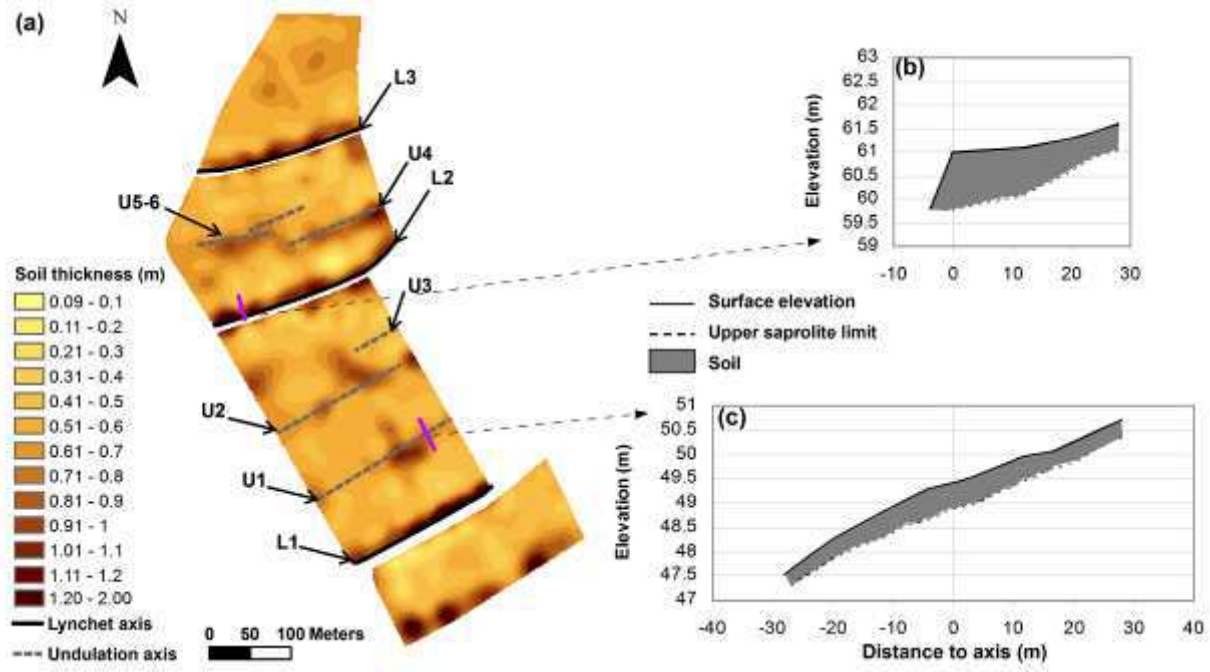

Figure 8. Soil thickness variability within the study area: (a) map of soil thickness estimated from the 586 points of the estimation dataset. Illustrations of characteristic topographic cross-section and soil thickness evolution (b) in a lynchet and (c) in an undulation.

3.2. Variability of the predictor variables in each expert class

Table 2 presents summary statistics of morphometric attributes and soil thicknesses for each class and their respective size in the total dataset. The total dataset contains 734 points distributed in the following three classes: class 0 (389 points), class 1 (139 points) and class 2 (206 points). Classes 1 and 2, which are dedicated to the linear landforms of interest, represent 19% and 28% of the total dataset, respectively.

Table 2. Summary statistics of morphometric attributes and soil thickness in each expert class.

Class	Size	Slope (%)			Curvature (m^{-1})*			Profile curvature (m^{-1})*			Planform curvature (m^{-1})*			Soil thickness (m)		
		Min	Mean (S.D**)	Max	Min	Mean (S.D**)	Max	Min	Mean (S.D**)	Max	Min	Mean (S.D**)	Max	Min	Mean (S.D**)	Max
0	389	0.84	6.04 (2.5)	11.90	-0.35	-0.02 (0.2)	1.18	-0.99	0.02 (0.2)	0.33	-0.20	0.00 (0.1)	0.30	0.22	0.45 (0.2)	1.30
1	139	0.16	2.62 (2.0)	9.35	-1.01	-0.20 (0.2)	0.32	-0.14	0.18 (0.2)	1.03	-0.30	-0.01 (0.1)	0.47	0.45	1.08 (0.4)	2.23
2	206	2.37	5.73 (2.2)	10.32	-0.32	0.05 (0.1)	0.36	-0.28	-0.04 (0.1)	0.33	-0.20	0.00 (0.1)	0.32	0.35	0.62 (0.2)	1.30

* The negative values of curvature and planform curvature mean for concavity and positive values for convexity. The negative values of profile curvature mean for convexity and positive values for concavity.

** S.D: Standard deviation.

According to the summary statistics (Table 2), class 0 presents the largest range of slope values (from 0.84% to 11.9%) and the highest mean slope value (approximately 6%). Mean values for each of the three curvatures calculated on undifferentiated surfaces (class 0) are null, with an S.D. of 0.1 to 0.2 m^{-1}. Class 1 presents the lowest mean slope value (2.62%) with a minimum and a maximum of 0.16% and 9.35%, respectively. Its mean value for planform curvature is null, as observed for classes 0 and 2. The profile curvature of class 1 appears mainly concave with a mean value of 0.18 m^{-1} (S.D. = 0.2 m^{-1}). Class 2 shows the highest minimal slope value (2.37%) and a mean slope value of 5.73%. The ranges of values for the three curvatures are the lowest in this class. Profile curvature varies from −0.28 to 0.33 m^{-1}.

The lynchets (class 1) present the most important mean measured value of soil thickness (1.08 m), and the largest range of soil thickness values (from 0.45 to 2.23 m; Table

2). The soil thickness variability appears higher perpendicularly to lynchets than along their axes. Solum systematically becomes thicker from the upslope to the downslope of a lynchet. A vertical section in this type of landform presents a soil accumulation with an approximated ight-angle triangle shape (Fig. 8b). According to Table 2, soil thickness in classes dedicated to undifferentiated surfaces and undulations (Classes 0 and 2) does not exceed 1.3 m. Class 2 shows higher minimal and mean soil thickness values than class 0. Mean values for classes 0 and 2 are 0.45 and 0.62 m, respectively. Soil also presents a particular evolution in undulations. A vertical cross-section in an undulation shows a slight convex lenticular thickening (Fig. 8c).

The Tukey HSD method was applied on the 734-point dataset (Table 3). This statistical test was used to find which ranges of values are significantly different from one another for a given predictor variable. The ranges of values related to classes 0, 1 and 2 are statistically different one from another for each of the following predictor variables: soil thickness, profile curvature and curvature. The classes 0 and 2 exhibit similar ranges of values for slope and planform curvature.

Table 3. Tukey's HSD (Honestly Significance Differences) test results (α level: 0.05).

Contrast	Slope	Curvature	Profil curvature	Planform curvature	Soil thickness
1 vs 0	Yes	Yes	Yes	Yes	Yes
1 vs 2	Yes	Yes	Yes	Yes	Yes
2 vs 0	No	Yes	Yes	No	Yes

3.3. Classification Tree Results

3.3.1. The Classification Tree CT_{soil}

The overall prediction performance of the CT method is more than 80% when applied to morphometric attributes and soil thickness values of the pre-classified calibration dataset (Table 4). The confusion matrix shows that the resulting regression tree CT_{soil} performs well for classes 0 and 1. Classes 0 and 1 have 87.5% and 85.0% of their respective points correctly classified. Approximately three-fourth of the misclassified points from class 0 are classified in class 2. Concerning class 1, the main errors of the model appear to involve class 0. In class 2, 24.0% of points are incorrectly classified; they are all allocated to class 0 by the model. The

most important risk of confusion during the application of the CT_{soil} model then involves classes 0 and 2.

Table 4. Confusion matrix on calibration dataset (CT_{soil} model).

Class	0'	1'	2'	Total	% correct*
0	279	11	29	319	87.5
1	12	85	3	100	85.0
2	40	0	127	167	76.0
Total	331	96	159	586	83.8

' means for estimated class.

* corresponds to the ratio of objects correctly classified within the class by the CT model.

Table 5 presents validation results for the CT_{soil} model performed through the validation dataset and the mapping of lynchets and undulations over the study area based on the decision rules of the concerned model (Fig. 9a). According to the validation procedure, 83.1% of the points from the validation dataset are correctly classified. Classes 0, 1 and 2 have 80.0%, 92.3% and 79.5% of their points correctly classified, respectively. The classification model CT_{soil} appears significantly relevant. Among points misclassified from the original class 0, confusions with classes 1 and 2 are almost equivalent. Six points are allocated to class 1, and eight points are allocated to class 2. Concerning class 2 (undulations), three-fourths of the misclassified points are confused with class 0 by the CT_{soil} model. Confusion between classes 0 and 2 appears to be the most important. This confusion explains why these classes present less efficient classification results than class 1.

Table 5. Validation procedure results from CT_{soil} model.

Class	0'	1'	2'	Total	% correct*
0	56	6	8	70	80.0
1	1	36	2	39	92.3
2	6	2	31	39	79.5
Total	63	44	41	148	83.1

' means for estimated class.

* corresponds to the ratio of objects correctly classified within the class by the CT model.

The mapping of the studied landforms based on the decision rules of CT_{soil} is shown in Fig. 9a. The three lynchets, L1, L2 and L3 (class 1), and five of the six sampled undulations, U1, U2, U4, U5 and U6 (class 2), are detected and mapped using the CT_{soil} model.

Unfortunately, some cells located in U3 are mapped as belonging to either class 1 or 0. A fourth linear lynchet landform, L4, is detected along the downslope site border. Three pseudo-linear areas (L5) appear in the northern part of the site. Several linear undulations (U7, U8 and U9) and undulation networks (U10) are identified by the CT_{soil} model. Axes of U8 and of some areas of U10 appear oriented along the main slope. Areas mapped in class 1 or 2 that are also not particularly linear and/or of decametric-scale are considered as classification errors.

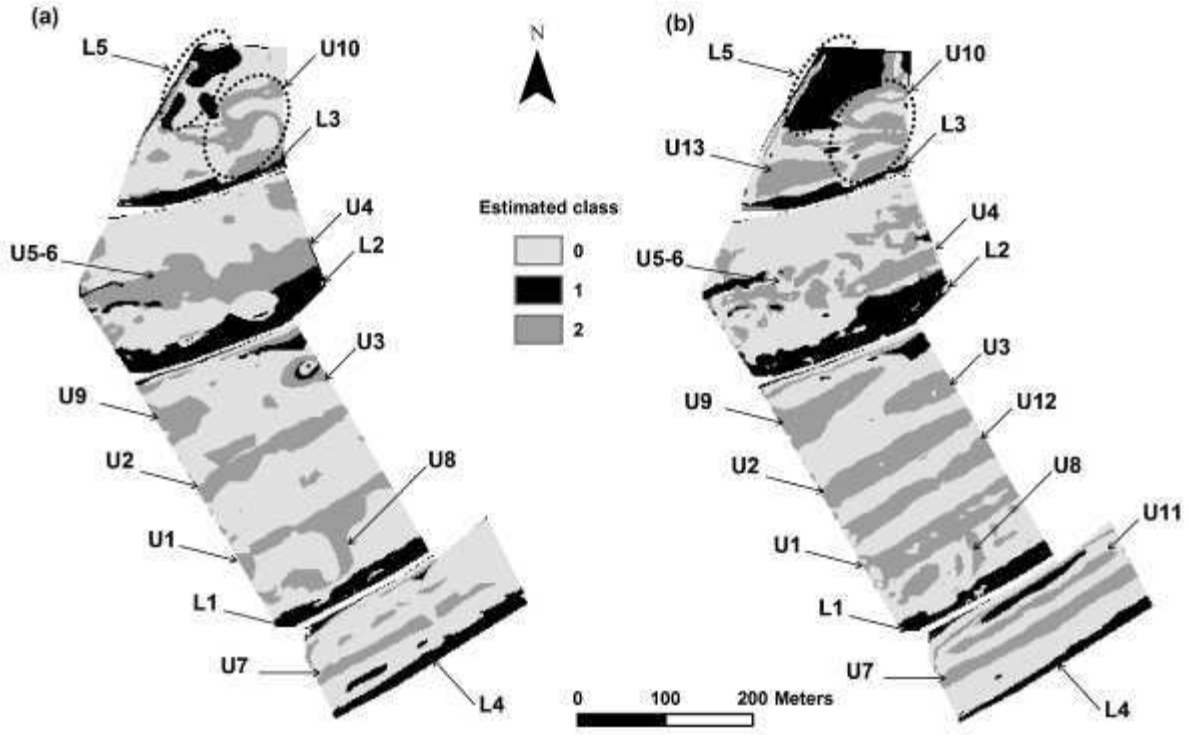

Figure 9. Maps of (a) CTsoil model and (b) CTtopo model results in the study area.

Class 0: undifferenciated area.

Class 1: lynchet.

Class 2: undulation.

3.3.2. The Classification Tree CTtopo

CT analysis on the basis of morphometric attributes was carried out in the outlook of spatial extrapolation beyond areas where the soil thickness variable is unavailable. The CART algorithm applied to the entire 586-point calibration dataset performs weakly when the soil thickness predictor variable is ignored (results not shown). This is mainly due to difficulties discriminating class 2 from class 0. However, the CART algorithm applied to the subset of the calibration dataset including only classes 1 and 2 (267 points from the total of 586 of the calibration dataset) performs better. The confusion matrix (Table 6) reveals that the individuals of each class are well classified. The overall performance is more than 96%. Only one point of 167 points from class 2 is allocated to class 1 by the CT_{topo} model, and eight of the 100 points from class 1 are allocated to class 2. Classes 1 and 2 can be efficiently discriminated one from another by morphometric attributes only.

Table 6. Confusion matrix on the subset of calibration dataset including only classes 1 and 2 (CT_{topo} model).

Class	1'	2'	Total	% correct*
1	92	8	100	92.0
2	1	166	167	99.4
Total	93	174	267	96.6

' means for estimated class.

* corresponds to the ratio of objects correctly classified within the class by the CT model.

Table 7 presents validation results for the CT_{topo} model performed through validation dataset and the mapping of lynchets and undulations over the study area based on the decision rules of the concerned model (Fig. 9b). Approximately 67% of the points from the validation dataset are well reclassified by the CT_{topo} model against 83% for the previous CT_{soil} model. A spatial extrapolation beyond the study area where the soil thickness variable is unavailable supposes an overall misclassification of approximately 30%. Regardless of the model used (CT_{topo} or CT_{soil}), lynchets are well identified in contrast to undulations. According to validation results, about 82% of points from class 1 and 59% of points from class 2 are well reclassified. Approximately 38% of points from class 2 are not recognised by the model as belonging to class 2, and are then automatically linked to class 0 by default. Nineteen of the 70 points of class 0 have morphometric attributes which correspond to the classification

criteria of class 2 defined by the CT_{topo} model. Confusion between classes 0 and 2 appears more important when soil thickness is not accounted for.

Table 7. Validation procedure results from CT_{topo} model.

Class	0'	1'	2'	Total	% correct*
0	44	7	19	70	62.9
1	5	32	2	39	82.1
2	15	1	23	39	59.0
Total	64	40	44	148	66.9

' means for estimated class.

* corresponds to the ratio of objects correctly classified within the class by the CT model.

The mapping of the studied landforms based on the decision rules of CT_{topo} shows that lynchets L1, L2 and L3 and undulations U1, U2 and U3 are recognized and mapped (Fig. 9b). Undulations U4 and U5–6 appear partially mapped, and L4, L5, U7, U8, U9 and U10 are detected. The spatial extent of the landforms differs from the CT_{soil} results, especially for undulations (class 2). Two additional linear areas are mapped in class 2 (U11 and U12) as well as non-linear areas (U13) located in the northern part of the site.

3.4. Volume of soil material stored in the anthropogenic landforms

Table 8 presents results concerning amounts of soil stored in lynchets and undulations. These calculations were made through the application of CT_{soil}, i.e., the most efficient classification model amongst CT_{soil} and CT_{topo}. According to the mapping of the studied landforms based on CT_{soil} decision rules (Fig. 9b), lynchets and undulations cover 14.3% and 24.3% of the total study area, respectively. The storage thickness t_i, defined through the computation of STh_{st} (Section 2.5), ranges from 0 m to 1.40 m in lynchets and from 0 m to 0.78 m in undulations. Volumes of soil material stored in these two types of anthropogenic landforms are approximately 6030 m^3 and 7520 m^3 for lynchets and undulations, respectively. Lynchets and undulations contain then approximately 15% of the total soil material present in the study area.

Table 8. Soil material accumulated in lynchets and undulations revealed by CT_{soil} model.

Type of landform	Accumulation area (m^2)	% of total study area	Storage thickness t_i (m)		Stored volume (m^3)	% of total soil material V_{st} in stuy area
			Min	Max		
Lynchets	22148	14.3	0.00	1.40	6031	6.6
Undulations	37856	24.3	0.00	0.78	7517	8.2

4. Discussion

The approach presented above aims to identify and distinguish two different types of linear landforms by morphometric attributes and soil thickness. The landforms detailed in the study area appear to be associated with soil thickenings. Therefore, their identification and distinction would allow a better appreciation of soil variability in cultivated hillslopes.

4.1. Classification efficiency

The classification method developed here is efficient using morphometric attributes and soil thickness (CT_{soil} model). Validation results of both classification models CT_{soil} and CT_{topo} (Tables 5 and 7, respectively) show that lynchets (class 1) and undulations (class 2) are well discriminated from each other with or without soil thickness. Both models perform well for the recognition of class 1. However, the undulations are less well identified than lynchets because of confusions between class 2 and class 0 (undifferenciated areas), especially when soil is not accounted for.

Class 1 is the only class that presents significant statistical differences for values of all the predictor variables when compared to the two others classes (Table 3). Lynchets show the highest profile curvature values corresponding to a marked concave shape (Table 2). The mean slope value (2.6%) barely reaches half of other class mean values, and its minimum slope is almost null. These statistics seem to reflect the consequent slope gentling associated with lynchet landforms (Fig. 3a,b) and which has been observed in other hilly agricultural regions in western Europe (Bracq and Delay; 1997; Salvador-Blanes, 2002; Follain, 2005; Houben, 2008; Brown, 2009). The lynchets studied here present larger soil thickness in comparison to undulations (respectively 1.1 and 0.6 m in mean thickness against 0.45 m in undifferentiated surfaces; Table 2). Like relief, soil thickness variability is more accentuated

perpendicular to the landform axis than along the axis. Soil thickness increases from upslope to downslope in lynchets (from a few decimetres to more than 1.5 m) by the way of a pseudo right-angle triangular accumulation (Fig. 8 b). This shape of soil explains the slope gentling characteristic to lynchet landforms. Lynchets are then easily identified statistically by both the CT_{soil} and CT_{topo} applications (approximately 92% and 82% of performance respectively, Tables 5 and 7).

The slope and planform curvature modalities of class 2 do not differ statistically from those of class 0 (Table 3). Thus, classes 0 and 2 are only distinguishable by curvature and profile curvature in the CT_{topo} application. Moreover, profile curvature values range from −0.99 to 0.33 m^{-1} and from −0.28 to 0.33 m^{-1} for classes 0 and 2, respectively (Table 2). The profile curvature does not help to distinguish classes 0 and 2 when its values for the class 0 are close to zero. An undulation is a more discrete and complex feature than a lynchet. Houben (2008) defined undulations as 'horizontal cylindrical segments', and thus highlighted the importance of their median convex areas (Fig. 3c,d). Class 2 statistics do not reflect a dominant convex trend (Table 3). Firstly, this major convex shape is systematically induced by a slight slope gentling upslope (a concavity). Secondly, it often ends also with a second slight concavity downslope. The presence of this second concavity depends on the difference between slope gradient of the undifferentiated areas located upslope and downslope to the undulation. Objects from classes 0 and 2 can then present similar combinations of morphometric attributes. This could explain why the CT_{topo} including the three classes did not significantly distinguish classes 0 and 2.

Soil thickness appears to be an important predictive variable for undulation landforms. We systematically observed a soil thickening in sampling profiles perpendicular to undulations, even a slight one (~10 cm). The thickening shows a convex lenticular shape (Fig. 8c). The mean soil thickness in undulations is 0.62 m vs. 0.45 m in undifferentiated areas (Table 2). The intensity of soil thickening in both lynchet and undulation landforms appears to vary along their axes and from one perpendicular sampling transect to another. These short-distance variations of a few to >20 cm seem to have no significant consequences on local relief when compared to the magnitude of relief variation in lynchets and undulations (Fig. 6). The C horizon upper limit probably presents local irregularities along the different landforms hidden by the shape of overlying thickened soils. In addition, a few subtle

undulation landforms (e.g., U5–6) appear associated with important soil thickening; this supports that the C horizon upper limit is necessarily mostly concave across the landform. In this particular case, the greater soil thickness helps identify undulations (Fig. 9a). Conversely, remarkable undulation landforms (e.g., U3) present slight soil thickening; this supports the idea that the C horizon upper limit is mostly convex across the landform. Consequently, the CT_{topo} model does not support the discrimination of classes 0 and 2 (Fig. 9b). These local variations of C horizon upper limit have a poor effect on the classification efficiency of class 1, considering its very distinctive landform attributes and important soil thicknesses.

4.2. The imprint of successive field border networks

Linear lynchet landforms have been described to result from the progressive soil material accumulation upslope of field borders (Bollinne, 1971; Papendick and Miller; 1977; Govers *et al.*, 1999; Salvador-Blanes, 2002; De Alba, 2003). Because undulations are linear and associated with thicker soils, they are also possibly related to ancient field borders. Moreover, lynchet and undulation landforms are both predominantly oriented perpendicular to the main slope. Nevertheless, undulation-like landforms can be related to other factors such as a natural increase in soil thickness and/or topographic variation of saprolite upper limit (Section 4.1). Outcropping limits between the underlying chalk and limestone beds appear to be perpendicular to the main slope (Alcaydé *et al.*, 1989). These sedimentary rocks have successive beds of metric-to-decametric-scale and of different compositions, hardnesses. These different rocks are more or less resistant to erosion: their outcroppings could then have influenced local topography and soil profile development. Unfortunately, there is no map of bedrock lithology accurate enough to assess the implication of lithology in the development of undulation landform here. On the contrary, information about historic field system layouts is available. Fig. 10 presents the mapping of lynchets and undulations over the study area performed from CT_{soil} model and combined with the field border networks that have been known since 1836. All the linear landforms surveyed in this study are spatially linked to field borders. Lynchets are constructed along present field borders, whereas undulations are located on ancient field borders.

The field borders associated with lynchets L1, L2 and L3 have existed since at least 1836 (Fig. 10). These limits are followed by perennial roads (L1 and L2) or access to the

fields (L3), which could have been present for decades to centuries before 1836. A fourth effective lynchet (L4), associated with the field border edging the alluvial plain, has been mapped by CT applications. The field border has existed since at least 1836, as those associated with L1, L2 and L3 (Fig. 10). In addition, soil in L4 thickens similarly to soil in lynchets L1, L2 and L3. Soil thickness in L4 varies from approximately 50 cm at 30 m upslope of the field border to up to 150 cm near the border (Fig. 8c). This footslope lynchet is recurrent on cultivated areas. The L5 areas are not located upslope of any known field borders. They are on the hillslope shoulder where the slope gradient is gentle and soils are locally more developed (due to a deeper weathering of the bed-rock in more flat areas). Thus, some areas can present predictor variables similar to class 1.

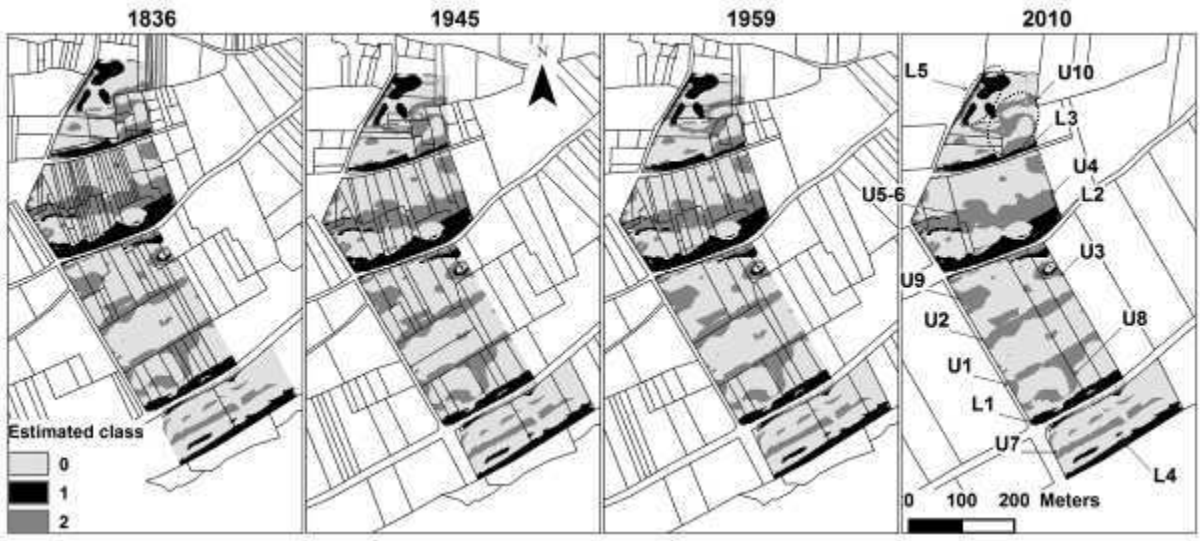

Figure 10. Maps of CTsoil model results and field border networks of 1836, 1945, 1959 and 2010.

Class 0: undifferenciated area.

Class 1: lynchet.

Class 2: undulation.

Undulations U1 to U6 are linked to field borders that have existed since at least 1836, and disappeared during the last campaign of land consolidation in 1967 (Fig. 10). Some cells of U3 are mapped as belonging to classes 1 or 0 by CT_{soil} (Fig. 9). U3 presents thinner soils than other undulations, but appears morphologically well-developed (Figs. 6 and 8a). Because some ranges of morphometric attribute values are intersected from one class to the other (Table 2), slight soil-thickness variations do not support the identification of U3 as

undulations by CT_{soil}. U9 is linked to a former field border that existed since at least 1836 and disappeared between 1946 and 1958. The geometrical network U10 is associated with successive borders that were very close to one another and had similar orientations. These borders disappeared after 1959. Undulations U7 to U10 were evidenced by both classification models and U12 by CT_{topo} only (Fig. 9). These five undulations are weakly developed in the field. Their associated field borders disappeared earlier than those linked to undulations which are better developped (U1 to U6). All of these undulations are linked to former field borders, have variable widths, and are roughly asymmetric.

The following two scenarios seem possible concerning the origin of these undulations: i) the undulations are former lynchets that were more or less developed and have been levelled after their associated field borders were destroyed, as suggested by Bollinne (1971) and Houben (2008). The soil material redistribution could have occured up- and downslope these landforms (Revel and Rouaud, 1985; Walling and Quine, 1991); ii) undulations are headlands created by an asymmetric accumulation of soil due to tillage translocation on both sides of the borders (Callot, 1980; Leturcq, 2008). Headlands have been mainly studied by the archaeology community in plains of northwestern Europe; they are more developed in planar context. They are often associated with field border networks created during the Middle Ages and have been active for several decades to a few centuries (Zadora-Rio, 1991; Leturcq, 2008; Brown, 2009).

U7 and U11 are not related to any known field border (U11 being revealed by CT_{topo} only; Fig. 9). These linear landforms can be linked either to borders that disappeared before 1836 or to a specific management (e.g., repeated paths of tillage implement). Concerning the undifferentiated surfaces (Class 0), these areas could correspond either to locations where no field border has ever been established, or to former lynchets or undulations erased since the removal of associated borders.

Lynchet and undulation axes are predominantly perpendicular to the slope. Field borders are an efficient place to block soil material fluxes that are controlled totally (running water) or partially (tillage) by gravity (Van Dijk *et al.*, 1996; Dabney *et al.*, 1999). The mapping of lynchets and undulations through the application of CT_{soil} or CT_{topo} model revealed some undulations oriented in the slope direction (U8 and in the U10 undulations

network, Fig. 10). In that case, only tillage erosion can explain an effective soil accumulation along those associated former borders. Tillage translocation is controlled first by the passage of the implement through the soil and then by the gravity effect (Lindstrom *et al.*, 1990; Van Muysen *et al.*, 2002). In the case of contour-line tillage, soil matter deposition occurs when tillage implements encounters field border oriented in the slope direction. This tends to suggest that U8 and U10 could be headlands originally.

Considering discussion in this section and Section 4.1, we synthesize the informations about field borders and possible origins of the linear anthropogenic landform studied here in the Table 9. The possible origins concern: i) the soil accumulation processes before any field border removal and; ii) the influence of the C-horizon upper limit on the actual landform morphology in comparison with soil accumulation.

Table 9. Anthropogenic linear landforms, associated field borders and possible origins.

Anthropogenic linear landform	Association with a known field border	Field border duration		Possible soil deposition processes	Possible substrate top influence
		From*	To**		
L1	Yes	min. 1836	present	Water + Tillage	?
L2	Yes	min. 1836	present	Water + Tillage	?
L3	Yes	min. 1836	present	Water + Tillage	?
L4	Yes	min. 1836	present	Water + Tillage	?
U1	Yes	min. 1836	1967	Water + Tillage	Yes
U2	Yes	min. 1836	1967	Water + Tillage	Yes
U3	Yes	min. 1836	1967	Water + Tillage	Yes
U4	Yes	min. 1836	1967	Water + Tillage	No
U5	Yes	min. 1836	1967	Water + Tillage	No
U6	Yes	min. 1836	1967	Water + Tillage	No
U7	No	?	?	Tillage	?
U8	Yes	min. 1836	1837-1944	Tillage	?
U9	Yes	min. 1836	1946-1958	Water + Tillage	?
U10	Yes	min. 1836	1967	Tillage	?
U11	No	?	?	Tillage	?
U12	Yes	1837-1944	1946-1958	Water + Tillage	?

* min. 18XX = date of the map where the border was mentioned for the first time.

** 19XX-19YY: a date between 19XX and 19YY.

4.3. Implications in soil mapping

Results show that spatial variability of morphometric attributes and soil thickness is strongly influenced by successive field border networks in the study area. Each of the three landform classes identified here presents a distinguishable range of soil thickness values. Lynchet and undulation landforms correspond to thicker soil due to material deposition alongside present or former field borders (Section 4.2). Soil accumulation viewed in vertical section evolved as a pseudo right-angle triangle in lynchets and as a convex lens in undulations. The method developed here has the convenience of mapping the classification results. Therefores, this method could improve the spatial estimation of soil thickness variations and related soil properties over cultivated landscapes.

The CART algorithm applied to morphometric attributes and soil thickness (CT_{soil}) performs well for lynchet and undulation discrimination. Without soil thickness, the algorithm correctly identifies lynchets apart from undulations (CT_{topo}). However, similarities between maps performed from CT_{soil} and CT_{topo} smodels represent approximately 70% of the study area. Half of the dissimilarities are estimated as class 0 by the CT_{soil} model and as class 2 by the CT_{topo} model. Approximately 7% of these dissimilarities are affected to the opposite possibility. Thus, the CT_{topo} model tends to overestimate undulation areas in comparison with the more accurate CT_{soil} model (Section 4.2). We note that CT_{topo} correctly detects the location of all the features studied here (Fig. 11). Both applications appear to be good tools for the recognition and mapping of the studied anthropogenic landforms within cultivated hillslopes, especially lynchets.

The different applications of CART algorithm performed in this study demonstrate the importance of relations between soil thickness variations and lynchet and undulation landforms. Although these linear landforms are discrete in the landscape, they cover a significant part of the study area. According to the mapping performed with CT_{soil} model (Table 8 and Fig. 10), lynchets and undulations cover approximately 14% and 24% of the 16 ha site area, respectively. This means that almost 40% of the site area shows morphological evidence of an effective human impact on the spatial variability of soils. Lynchets and undulations appear as morphological indicators of human-induced soil accumulations.

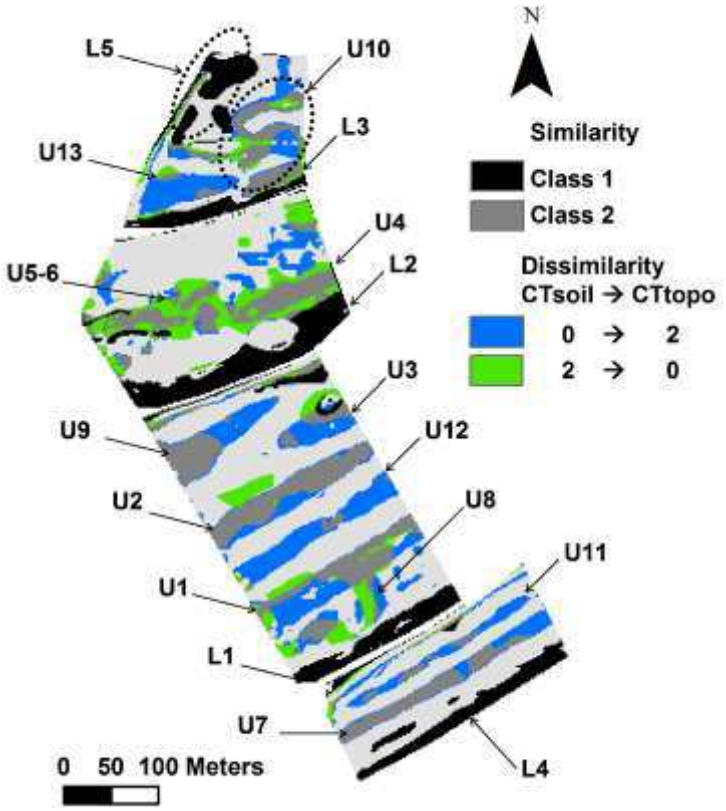

Figure 11. Map of similarity/dissimilarity from CTsoil model against CTtopo model results in study area.

Lynchets and undulations revealed by the CT_{soil} model contain about 6030 m^3 and 7517 m^3 of additionally stored soil material, respectively (Table 8). These volumes represent 6.6% and 8.2% of the total soil material present in the study area. More than 6030 m^3 of soil material could be then available to water and tillage translocations in this hillslope if field borders associated with current lynchets were destroyed in the immediate future. Although undulations are more discrete landforms than lynchets, they contain an equivalent volume of additionally stored soil material. Because undulations are associated with former field borders and lynchets to unchanged borders, undulations appear more frequently in the west of Europe. Politics, mechanisation and many other factors indeed stimulated important field border removal by land consolidation during the 1960s to 1980s in Western Europe (Vitikainen, 2004). These undulation landforms could be preferential areas for soil erosion by tillage, as wide gentle convexities within the landscape. Indeed, net soil loss by tillage translocation was demonstrated as being dependent on slope gradient changes. Erosion occurs on a convex slope, accumulation occurs on concave slopes, and a simple translation occurs on linear slopes (Lindstrom *et al.*, 1992, Govers *et al.*, 1996).

5. Conclusion

The aim of this study was to assess whether different types of anthropogenic landforms could be discriminated by their morphometric attributes and soil thicknesses. For this purpose, we developped a classification method based on a detailed field study carried out in a cultivated hillslope of the SW Parisian Basin (France). This method appears convenient because the classification models computed by the CART algorithm can be used as mapping tools.

We distinguished two different types of linear anthropogenic landforms in the study area, lynchets and undulations. They are easily distinguishable one from another by their morphometric attributes. Their ranges of soil thicknesses appear also statistically different: soil thicknesses are higher in lynchets than in undulations. These thicknesses are higher than those encountered in surrounding undifferentiated surfaces. Additionally, the shape of soil accumulation appears particular to each type of linear landform.

In contrast to lynchets, undulations are not easily distinguishable from undifferentiated surfaces by considering only morphometric attributes. Therefore, the distinction of undulations is less accurate than the distinction of lynchets. However, the undulation mapping is greatly improved when soil thickness is accounted for as predictor variable in the classification method.

Multi-temporal mapping of historic field system layouts shows that lynchets are associated with present field borders that have been established since at least 1836. The mapped undulations are linked to field borders that existed for a shorter time period and disappeared predominantly during the last campaign of land consolidation in 1967. Undulations appear to correspond to anthropogenic soil accumulations as lynchets. In perspective, the use of tracers as Cs-137 (half-time life of approximately 30.2 years) coupled to soil erosion modeling could be useful to precise the dynamics of both lynchet and undulation landforms since this last land consolidation.

Lynchets and undulations are rarely accounted for in landscape and regional-scale soil surveys. However, undulations are discrete and common linear landforms which can store an important amount of soil material. Our results would provide new perspectives in the soil

mapping discipline if associated with new technologies for relief recording. For example, the LIDAR (LIght Detection And Ranging) allows the accurate recording of high-density topographic data in large areas (Brown *et al.*, 2009; Rayburg *et al.*, 2009). Such technologies are of particular interest for quick soil mapping techniques with fine resolution. LIDAR could be very efficient to detect lynchets and undulations in the landscape.

Based on an analysis of morphometric attributes of some representative anthropogenic landforms linked with soil thickening, the method developed here could improve the spatial estimation of soil thickness variations and related soil properties over large areas.

Acknowledgements

Financial support provided by the ANR (Agence Nationale de la Recherche) VMCS project LANDSOIL is gratefully acknowledged. The authors would like to thank Jean-Paul Bakyono and Isabel Pene-Galland for data collection in the field. This paper was much improved thanks to the comments of Peter Houben and an anonymous referee and thanks to Lauren Valverde who revised my english style.

References

Alcaydé, G., Coubès, J., Macaire, J.-J., 1989. Feuille Loudun (513), Carte géologique de la France (1:50000), Orléans, BRGM.

Bellemlih, S., 1999. Stocks particulaires holocènes et bilans de matières dans un bassin fluviatile en domaine sédimentaire - Le bassin du Négron, Sud-ouest du Bassin Parisien, France. Ph.D. thesis, Université de Tours, France.

Bolliger, J., Wagner, H.H., Turner, M.G., 2007. Identifying and quantifying landscape patterns in space and time. In: Kienast, F., Wildi, O., Ghosh, S. (Eds.), A Changing World: Challenges for Landscape Research. Springer, Dordrecht, pp. 177-194.

Bollinne, A., 1971. Les rideaux en Hesbaye gembloutoise - Etude morphologique et sédimentologique. Bulletin de la Société géographique de Liège 7, 61-67.

Bourennane, H., 1997. Etude des lois de distribution spatiale des sols de Petite Beauce Application à la cartographie d'un horizon par couplage de méthodes morphométriques et géostatistiques. Ph.D. thesis, Université d'Orléans, France.

Boutin, D., Froger, D., Rassineux, J., 1990. Feuille Loudun (1724-1624), Carte des sols du Département de la Vienne et de la région Centre au 1:50000, Chambre d'Agriculture de la Vienne - IGN - INRA.